




# DNA Methylation in the Anti-Mullerian Hormone Gene and the Risk of Disease Activity in Multiple Sclerosis

Antonino Giordano, MD, PhD <sup>1,2,3</sup> Béatrice Pignolet, PhD,<sup>4,5</sup> Elisabetta Mascia, PhD,<sup>1</sup> Ferdinando Clarelli, MSc,<sup>1</sup> Melissa Sorosina, PhD,<sup>1</sup> Kaalindi Misra, PhD,<sup>1</sup> Florence Bucciarelli, MSc,<sup>4</sup> Laura Ferrè, MD, PhD,<sup>1,2</sup> Lucia Moiola, MD,<sup>2</sup> Roland Liblau, MD, PhD,<sup>4,6</sup> Massimo Filippi, MD <sup>1,2,3</sup> and Federica Esposito, MD, PhD <sup>1,2</sup>

**Objective:** Multiple sclerosis (MS) has a complex pathobiology, with genetic and environmental factors being crucial players. Understanding the mechanisms underlying heterogeneity in disease activity is crucial for tailored treatment. We explored the impact of DNA methylation, a key mechanism in the genetics-environment interplay, on disease activity in MS.

**Methods:** Peripheral immune methylome profiling using Illumina Infinium MethylationEPIC BeadChips was conducted on 249 untreated relapsing–remitting MS patients, sampled at the start of disease-modifying treatment (DMT). A differential methylation analysis compared patients with evidence of disease activity (EDA) to those with no evidence of disease activity (NEDA) over 2 years from DMT start. Utilizing causal inference testing (CIT) and Mendelian randomization (MR), we sought to elucidate the relationships between DNA methylation, gene expression, genetic variation, and disease activity.

**Results:** Four differentially methylated regions (DMRs) were identified between EDA and NEDA. Examining the influence of single nucleotide polymorphisms (SNPs), 923 variants were found to account for the observed differences in the 4 DMRs. Importantly, 3 out of the 923 SNPs, affecting DNA methylation in a DMR linked to the anti-Mullerian hormone (AMH) gene, were associated with disease activity risk in an independent cohort of 1,408 MS patients. CIT and MR demonstrated that DNA methylation in AMH acts as a mediator for the genetic risk of disease activity.

**Interpretation:** This study uncovered a novel molecular pathway implicating the interaction between DNA methylation and genetic variation in the risk of disease activity in MS, emphasizing the role of sex hormones, particularly the AMH, in MS pathobiology.

ANN NEUROL 2024;96:289–301

Multiple sclerosis (MS) is an immune-mediated neurodegenerative disorder of the central nervous system and a major cause of disability in young individuals.<sup>1</sup>

Despite significant advances in the understanding of the pathobiology of MS, it is still unclear what underlies the heterogeneity of disease severity in MS, that ranges

View this article online at [wileyonlinelibrary.com](https://www.wileyonlinelibrary.com). DOI: 10.1002/ana.26959

Received Jan 26, 2024, and in revised form Apr 17, 2024. Accepted for publication Apr 24, 2024.

Address correspondence to Dr. Federica Esposito, Human Genetics of Neurological Disorders Unit, Division of Neuroscience, IRCCS San Raffaele Scientific Institute, Via Olgettina 60, 20132 Milan, Italy, E-mail: [esposito.federica@hsr.it](mailto:esposito.federica@hsr.it)

From the <sup>1</sup>Division of Neuroscience, IRCCS San Raffaele Scientific Institute, Milan, Italy; <sup>2</sup>Department of Neurology and MS Center, IRCCS Ospedale San Raffaele, Milan, Italy; <sup>3</sup>Università Vita-Salute San Raffaele, Milan, Italy; <sup>4</sup>Toulouse Institute for Infectious and Inflammatory Diseases (Infinity), University of Toulouse, CNRS, INSERM, Toulouse, France; <sup>5</sup>Neurosciences Department, Toulouse University Hospital, Toulouse, France; and <sup>6</sup>Department of Immunology, Toulouse University Hospitals, Toulouse, France

Additional supporting information can be found in the online version of this article.

from patients with a relatively benign disease course to patients experiencing severe disability accumulation early from onset.<sup>2</sup> Gaining knowledge on the mechanisms underlying disease course heterogeneity in MS is crucial to have meaningful markers that can help a tailored treatment and drive future drug development.

DNA methylation, the addition of a methyl group ( $-CH_3$ ) at cytosine-phosphate-guanine (CpG) sites, is 1 of the most stable and studied epigenetic hallmarks across species.<sup>3</sup> Generally, methylation of CpG dinucleotides in enhancers and promoters leads to silencing of gene expression, while methylation occurring in the gene body is usually linked to increased expression.<sup>4</sup> The study of DNA methylation is very promising when studying complex diseases, as it is a key element in the crosstalk between genetics, environment, and gene expression,<sup>3</sup> and it has led to a deeper understanding of tumorigenesis and cancer transformation mechanisms.<sup>5</sup> The interplay between genetic and environmental factors is crucial for MS as well,<sup>6</sup> therefore making DNA methylation a relevant target in investigations on the pathobiology of the disease. For this reason, in the past few years the study of DNA methylation has greatly expanded in MS,<sup>7</sup> and many works showed that changes in DNA methylation occur in MS patients compared to healthy controls, both in bulk tissue<sup>8,9</sup> and isolated cell types.<sup>10,11</sup> In particular, DNA methylation has been found to mediate the human leukocyte antigen (HLA) system-related risk of MS,<sup>12</sup> but it is not known whether it is also involved in mechanisms linked to disease activity.

In this work, we investigate the impact of DNA methylation changes on disease activity, assessed by the no evidence of disease activity-3 (NEDA-3) status, in a bi-centric cohort of relapsing–remitting MS patients.

## Materials and Methods

### Study Cohort for Methylation Analysis

We included patients with diagnosis of relapsing–remitting MS (RR-MS) from 2 different centers: IRCCS San Raffaele Scientific Institute in Milan, Italy (OSR) and Toulouse University Hospital, France (CHUT). All patients were untreated at the time of blood sampling. After sampling, patients started disease-modifying treatments (DMTs) (interferon, glatiramer acetate, teriflunomide, or dimethyl fumarate) and underwent routine clinical follow-up. Patients previously treated with highly effective DMTs (natalizumab, S1P modulators, anti-CD20 drugs, alemtuzumab) or immunosuppressive drugs (azathioprine, mycophenolate mofetil, mitoxantrone, cyclophosphamide) were excluded to avoid heterogeneity in terms of observed disease activity in the study cohort. We also excluded patients with exposure to corticosteroid drugs in the 30 days prior to sampling to minimize a potential effect on methylation and gene expression.

Patients were classified as NEDA when all the following criteria were fulfilled over the 2-year follow-up: (1) no new relapses; (2) no new/enlarging or gadolinium enhancing lesions at brain and spinal cord MRI; (3) no Expanded Disability Status Scale (EDSS) progression. All patients had undergone clinical visits with MS specialists at each center at baseline and at least at month 12 and 24 from baseline, as per clinical routine. All MRI examinations were performed on 1.5 Tesla scanners and included T1-weighted (pre- and post-gadolinium administration), T2-weighted and fluid attenuated inversion recovery (FLAIR) sequences, as per clinical routine assessment. The definition of MRI activity was performed at each center by neuroradiologists and, when available, the images were double-checked by independent raters (A.G., F.E., R.L.) for the purpose of this study. Disability progression was defined as follows: an increase in the EDSS score of at least 1.5 if baseline EDSS was 0; an increase of at least 1.0 if baseline EDSS was between 1.0 and 5.5 points; an increase of EDSS of at least 0.5 if baseline EDSS was  $\geq 6.0$ .

### Methylation Analysis

**PBMC Extraction and Methylation Profiling.** After blood sampling, peripheral blood mononuclear cells (PBMC) were extracted through density gradient centrifugation by Lymphoprep™ (STEMCELL Technologies, Vancouver, Canada), as described in the manufacturer's protocol. DNA from PBMC was extracted using Quick-DNA/RNA Miniprep Plus (Zymo) for the OSR cohort and the Allprep DNA/RNA/miRNA Universal kit (Qiagen) for CHUT, according to the manufacturing protocols. Bisulphite conversion and methylation profiling was performed at the Laboratory of Human Genetics of Neurological Disorder at OSR. Randomization for array slides and position, controlling for relevant factors (the NEDA-3 status and center), was carried out to minimize potential batch effect (Table S1). After bisulphite conversion with the EZ DNA Methylation kit (Zymo), whole-genome methylation profile was obtained by means of Illumina Infinium MethylationEPIC BeadChips (Illumina, Inc., San Diego, CA, USA), following the manufacturer's instructions.

**Quality Control and Processing of Methylation Data.** Quality control (QC) was performed to remove probes according to the following criteria: probes with a detection  $p$ -value  $> 0.01$  in more than 5% of the subjects, non-CpG probes, X and Y chromosome probes, cross-reactive probes, probes mapping to known single nucleotide polymorphisms (SNPs), probes with less than 3 bead counts in at least 5% of the subjects.<sup>13</sup> No issues were detected during QC on samples when checking for sex or age mismatch and overall sample quality. A detailed QC report is provided in Table S2.

Within-array normalization and normalization for type I and II probes was performed using the *ssNoob* method, implemented in the *minfi* pipeline.<sup>14</sup> Methylation M-values were calculated, to be used in statistical analysis. We run a principal component analysis (PCA) on methylation using the FactoMineR pipeline,<sup>15</sup> and detected a batch effect exerted by methylation slide and position in the slide, as expected.<sup>16,17</sup> Therefore, we applied a batch correction using an empirical Bayes method by the means of the *ComBat* function implemented in the *SVA* package in R, which reduces error estimates and improves reproducibility.<sup>18</sup>

Since cellular heterogeneity may have a confounding effect on methylation levels, we obtained estimated cell proportions based on methylation beta-values using a reference-free deconvolution approach, implemented in the *EpiDISH* package.<sup>19</sup> Cell-proportions (CD8 T cells, CD4 T cells, NK cells, B cells, monocytes, and neutrophils) were incorporated as covariates in the subsequent analysis, to minimize the impact of cell fractions on differential methylation. After QC, all 249 subjects (OSR: 75, CHUT: 174) with RR-MS and a total of 778,879 probes were retained.

**Differential Methylation Analysis.** The *limma* R package<sup>20</sup> was used to fit generalized linear models assessing the relationship between DNA methylation and NEDA-3 status, using sex, age at disease onset, center, and cell type proportions as covariates. Significance of association for the resulting differentially methylated positions (DMP) was estimated at 5% false-discovery rate (FDR) following Benjamini-Hochberg procedure.

From the DMP, we derived the differentially methylation regions (DMR) using the *DMRcate* pipeline.<sup>21</sup> We used standard parameters (kernel bandwidth  $\lambda = 1,000$ , scaling factor  $C = 2$ ), to detect DMR encompassing a minimum of 3 CpGs, with at least a 2% change in methylation beta-values.

**Gene Ontology Enrichment Analysis.** Enrichment for gene ontology (GO) terms (category 'Biological process') was assessed using the top 100 mapped genes from the DMP analysis. The analysis was conducted using WebGestalt,<sup>22</sup> with standard settings.

### **Effect of Genotype on DNA Methylation and NEDA-3 Status**

**Methylation Quantitative-Trait-Loci Effect Study.** The methylation quantitative trait loci (mQTL) effect in PBMC was calculated in patients from the methylation analysis that also had available genotype information, obtained as described below.

All the SNPs mapping to a  $\pm 500$  kilobases (kb) window from the CpGs belonging to each of the identified DMR were tested. The association between SNPs and methylation M-values for CpGs was computed using linear modelling, and adjusting for biological sex, age at sampling, technical factors (array and array position, bisulphite conversion plate and plate position), and estimated cell proportions (neutrophils, monocytes, NK, CD8 T cells, CD4 T cells, B cells). To adjust for multiple testing, PLINK v1.9<sup>23</sup> was used to calculate the number of linkage disequilibrium (LD) blocks in each of the studied regions in the 1,000 Genomes project subjects of European ancestry<sup>24</sup> and Bonferroni correction (0.05/number of LD blocks) was applied. To calculate the LD blocks, the Haploview's interpretation of block definition, as integrated in PLINK v1.9, was used.<sup>25</sup>

**Genotyping and Imputation.** All the genetic data for the OSR cohort were extracted from a larger cohort of MS patients available at the Laboratory of Human Genetics of Neurological Disorders at IRCCS San Raffaele Scientific Institute. Individuals had been genotyped on 4 different platforms (Illumina OmniExpress, Illumina Omni 2.5, Illumina Human Quad and Illumina Global Screening Array). Patients from Toulouse had been genotyped on 2 different platforms: Axiom Genome-Wide LAT 1 (Affymetrix, USA), performed at CHUT, and Illumina OmniExpress, performed at OSR. The clinical features of the cohort undergoing genetic QC and analysis are reported in Table S8.

For OSR, imputation against reference genome (Haplotype Reference Consortium<sup>26</sup>) was carried out separately on each platform on Michigan Imputation Server with later merging on bona-fide imputed variants (imputation score  $R_{sq} > 0.6$ ). Given the high level of overlap between OmniExpress and Omni2.5, samples genotyped on these 2 platforms were jointly quality-controlled and imputed. Variants' rsIDs were assigned from dbSNP v151 GRCh37p13. Prior to imputation, a set of homogeneous QC steps at sample and SNP levels were conducted. At sample level, we excluded subjects with sex mismatch, those with call-rate  $< 90\%$  and outliers exceeding the mean level of heterozygosity by  $> 3$  standard deviations. At variant level, we discarded rare SNPs with allele frequency  $< 1\%$ , SNPs with a call-rate  $< 90\%$  and those departing from Hardy-Weinberg equilibrium at  $p < 1 \times 10^{-6}$ . To identify individuals with potential biological relationship in the study cohort, we performed a pairwise identical by descent estimate, that found 5 pairs of subjects with potential relatedness ( $PI\_HAT \geq 0.250$ ). Two pairs were excluded for  $PI\_HAT \geq 0.50$  and of the remaining 3 pairs, the individuals who were the least characterized were removed

(total number of individuals removed: 7). To identify population outliers, we run a PCA and outliers were excluded (mean  $\pm$  6 standard deviations). As an additional level of QC for the study cohort, we retained only SNPs with a call rate  $\geq$ 0.99 and minor allele frequency (MAF) of at least 5%. A PCA on the final dataset was also run to use principal components (PC) as covariates in the subsequent association analysis. The final dataset included 1,154 subjects and 4,231,855 variants.

For CHUT, the imputation was carried out separately, as described for the OSR cohort. Post-imputation QC were performed as reported for the OSR cohort. For CHUT, starting from 299 patients, 7 were excluded for heterozygosity rate, 1 for IBD, 27 for PCA, and 20 identified as of non-Caucasian ancestry, resulting in a total of 254 subjects and 5,127,516 SNPs were retained after the QC.

**Association Analysis with the NEDA-3 Status.** The genetic association analysis with the NEDA-3 status was conducted on a larger cohort of individuals with available whole-genome data obtained as described above (Table S8). From this cohort, we extracted the subjects who fulfilled the clinical inclusion criteria to define the NEDA-3 status at 2 years from the start of first-line DMT. From whole-genome data, we extracted the SNPs with evidence of mQTL effect on the DMR and studied their impact on disease activity. The 2 cohorts (OSR and CHUT) were first analyzed separately using PLINK v1.9.<sup>23</sup> Logistic regression was carried out using the NEDA-3 status as outcome and genotype as predictor. To select the covariates for logistic regression model we conducted a preliminary exploratory analysis between clinical and demographic factors and the NEDA-3 status. Sex, age, and PC 1 to 8 were included in the OSR cohort as covariate. In the CHUT cohort PC1 and PC2, age and sex were included as covariates. The genetic association analysis was conducted calculating the odds ratio (OR) of reaching the NEDA-3 status given by the A1 allele (effect allele). After the 2 single-cohort analysis, the results were meta-analyzed using a fixed-effect model with PLINK v1.9, retaining only the variants that were common to both cohorts.

To account for multiple testing, we again applied a Bonferroni correction on the number of LD blocks (calculated as described above) in the tested SNP for each independent region.

### Causal Inference Test

To explore whether DNA methylation is the mediator of the genetic risk of disease activity, we used causal inference test (CIT), as previously reported,<sup>12,27</sup> as it is a robust method to

overcome pleiotropy and reverse confounding effects in complex diseases as MS. The analysis was run on the subset of patients of the main methylation cohort that had available genotype (n = 231). We run CIT using the SNPs with evidence of effect both on methylation and disease activity, modeling the NEDA-3 status as phenotype and the methylation beta-values as a mediator.

### Effect of Genotype on Gene Expression

The expression-QTL (eQTL) effect in PBMC was evaluated on a subgroup of the MS patients included in the methylation analysis, that had available whole-genome gene expression and genotype data (n = 225). Inclusion criteria and PBMC extraction were described above. RNA from PBMC was extracted using Quick-DNA/RNA Miniprep Plus (Zymo), according to the manufacturing protocol. Quantity and quality of RNA was assessed by Qubit (Thermo Fisher Scientific) and TapeStation (Agilent Technologies). The transcriptomic profile of patients was obtained via next-generation sequencing at CHUT. RNA libraries were generated using the TruSeq Stranded mRNA Library Prep Kit (Illumina) and sequenced on a HiSeq3000 sequencer (Illumina), reaching >25 million reads/samples on average. RNA-seq reads were aligned to hg19 reference genome, removing poor-quality bases and adapter sequences. Quantification of gene expression levels and feature-level summarization was performed using featureCounts,<sup>28</sup> according to GENCODE v19 annotation gene model. Quality control of raw and aligned reads was performed by means of MultiQC tool.<sup>29</sup> To discard features deemed as not expressed, we only retained those with >5 counts in at least 25% of the whole cohort. From transcriptome-wide analysis, we extracted the gene of interest and computed the eQTL effect between the genotype of the studied SNPs (obtained as described above) and rank-inverse transformed normalized gene counts (via linear modelling, adjusting for center, age at sampling, and sex).

### Mendelian Randomization

We run Mendelian randomization (MR) analysis to assess whether DNA methylation is causally associated with change in gene expression. First, we applied a pruning for LD ( $R^2 > 0.3$ ) using 1,000 Genomes European population<sup>24</sup> as a reference on the 3 SNPs with evidence of mQTL effect that mediated the genetic risk of disease activity using CIT, as it is a prerequisite for MR that the variants are not strongly correlated. Then, we run a 2-sample MR analysis using an inverse-variance weighted model in the *MendelianRandomization* R package.

### Standard Protocol Approvals, Registrations, and Patient Consents

The study was approved by the local ethical committees at IRCCS San Raffaele Scientific Institute (Milan, Italy) and at Toulouse University Hospital (Toulouse, France).

## Results

### Differential Methylation Analysis Identified 4 Regions Associated with Disease Activity

A total of 249 RR-MS patients fulfilling the inclusion criteria were sampled for DNA methylation profiling before treatment start and underwent QC. Clinical data were collected retrospectively through revision of medical records and MRI to define the NEDA-3 status<sup>30</sup> at 2 years from treatment start (Table 1). In addition, for each site, a subset of the MRI studies was reviewed independently for quality assurance (OSR: 70/75, CHUT: 118/174). The clinical and demographic features of the patients who underwent methylation profiling and analysis are reported in Table 1. In these subjects, we carried out an analysis to unravel sites of the genome that are differentially methylated between patients without (NEDA) and with evidence of disease activity (EDA) over 2-year follow-up from first-line treatment start (Table 1). A flowchart of the analyses is shown in Figure 1A.

As a first step, we investigated single CpGs running a DMP analysis, as it is instrumental to the generation of DMR. The DMP analysis revealed that DNA methylation

levels of 7 CpGs at baseline were significantly associated with the NEDA-3 status at 2 years, after adjustment for multiple testing (FDR  $p < 0.05$ ) (Table 2). These sites overall map to genes with potential interesting effect on the immune system (see Discussion).

Then, to identify regions of contiguous CpGs associated with the outcome and provide a more biologically meaningful insight, we focused on the difference in methylation occurring in wider portion of the genome, deriving DMR from DMP. We successfully detected 4 regions that were differentially methylated between NEDA and EDA patients, as shown in Table 3.

### Genetic Variation Significantly Affects Methylation Levels

Genetic variation can extensively affect the levels of DNA methylation (i.e. methylation Quantitative-Trait-Loci effect, or mQTL effect).<sup>4</sup> To understand whether the difference in methylation observed in the 4 DMR is controlled by genetic factors, we studied the impact of SNPs in *cis* ( $\pm 500$  kb from each DMR) on the methylation levels of the CpGs composing each DMR in the PBMC

**Table 1. Clinical and Demographic Characteristics of Cohort for the Methylation Study Cohort**

Parameter	OSR	CHUT	Total	<i>p</i> -Value
No. of subjects	75	174	249	-
Age at sampling	37.1 (9.8)	40.1 (10.8)	39.2 (10.3)	0.04 <sup>†</sup>
Age at onset	32.7 (8.9)	33.4 (10.2)	33.2 (10.1)	0.68 <sup>†</sup>
F/M ratio	1.59	3.97	2.89	0.0021 <sup>§</sup>
Disease duration	4.3 (6.5)	6.6 (7.7)	5.9 (7.2)	0.046 <sup>†</sup>
EDSS score	1.5 (1.0–2.0)	1.5 (1.0–2.5)	1.5 (1.0–2.0)	0.13 <sup>†</sup>
NEDA status at 2 years				0.002 <sup>§</sup>
NEDA	29 (39%)	106 (61%)	135 (54%)	
EDA	46 (61%)	68 (39%)	114 (46%)	
DMT started at baseline				-
Dimethyl fumarate	68%	42%	50%	
Teriflunomide	16%	34%	29%	
Copaxone	13%	8%	9%	
Interferon-beta	3%	16%	12%	

*Note.* The total and center-specific characteristics of the study cohort at baseline are shown. In the rightmost column, the *p*-values from chi-square test (§) or Mann–Whitney–Wilcoxon test (†)—as appropriate—are reported, to identify baseline differences between the 2 centers. For age at sampling, age at onset and disease duration mean values (with standard deviation) are displayed. For the EDSS score, the median value and its interquartile range is shown. For the NEDA status at 2 years, the raw numbers are reported (with percentage).

Abbreviations: CHUT, Toulouse University Hospital; DMT, disease-modifying treatment; EDA, evidence of disease activity; F/M ratio, female/male ratio; OSR, IRCCS San Raffaele Scientific Institute.

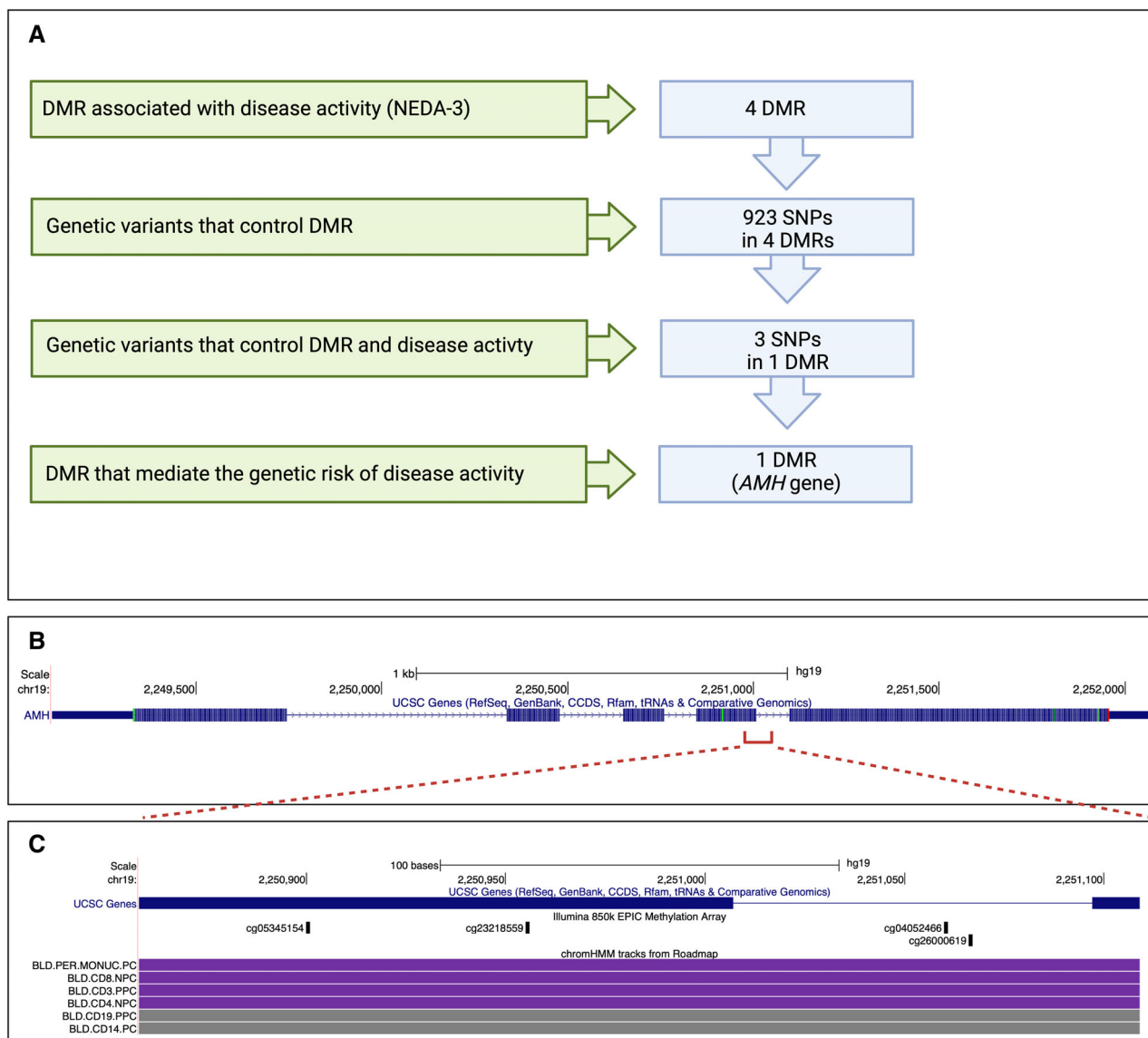


**FIGURE 1:** Flowchart and identification of DMRs. (A) The approach used to identify the causal relationship between methylation, genetic variation, and disease activity, as described in the main text. (B) The UCSC RefSeq track (GRCh37/hg19) for the *AMH* gene, with highlight (red brackets) of the identified DMR. (C) The DMR in the *AMH* gene (and the respective CpGs from the Illumina EPIC 850 K array) and RoadMap chromatin states<sup>31</sup> for PBMC (BLD.PER.MONUC.PC), T lymphocytes (BLD.CD3.PPC: CD3+ T cells, BLD.CD4.NPC: CD4+ T cells, BLD.CD8.NPC: CD8+ T cells), B lymphocytes (BLD.CD19.PPC: CD19), and monocytes (BLD.CD14.PC). The purple track indicates that the region is part of a bivalent promoter in PBMC and in CD4/CD8 T cells, while the dark gray track indicates that the region maps to a polycomb repressive complex in monocytes and B cells.<sup>31</sup> [Color figure can be viewed at [www.annalsofneurology.org](http://www.annalsofneurology.org)]

from the subgroup of patients with available genotype data ( $n = 231$ ) (Figure 1). We identified a total of 923 SNPs that exert a mQTL effect on the CpGs composing the 4 DMR, demonstrating a significant contribution of genetic variation (Tables S4–S7).

### Genetic Variation in *AMH* Affects Disease Activity

Since multiple SNPs were found to account for the difference in methylation between NEDA and EDA patients, it

is reasonable to expect that the same variants can also affect the risk of NEDA/EDA. Therefore, we assessed whether the SNPs influencing the levels of methylation in the 4 DMRs were also associated with disease activity in MS, taking advantage of a larger cohort composed by 1,408 patients from OSR and CHUT, and using the NEDA-3 status as outcome disease activity (Figure 1). Of the 923 SNPs exerting mQTL effect, we found that for only 1 DMR (DMR1, see Table 3), 3 variants regulating the methylation levels of DMR1 were also associated with

**TABLE 2. Top 20 DMPs**

CpG	LogFC	p-Value	Adj. P	CHR	BP	Gene	Gene Feature
cg27267436	-0.2	6.42 x 10 <sup>-8</sup>	0.046	19	3,754,012	APBA3	Body
cg20025086	0.11	1.65 x 10 <sup>-7</sup>	0.046	12	109,569,130	Intergenic	IGR
cg20308351	0.21	1.77 x 10 <sup>-7</sup>	0.046	7	3,067,980	CARD11	5'UTR
cg22193657	0.09	2.61 x 10 <sup>-7</sup>	0.046	3	194,948,010	XXYL1	Body
cg19915997	-0.16	3.61 x 10 <sup>-7</sup>	0.046	3	15,492,725	COLQ	3'UTR
cg25829490	0.18	4.00 x 10 <sup>-7</sup>	0.046	2	176,988,792	HOXD9	Body
cg12362502	-0.22	4.16 x 10 <sup>-7</sup>	0.046	6	43,603,544	MAD2L1BP	TSS200
cg07146435	0.12	6.45 x 10 <sup>-7</sup>	0.061	10	100,028,499	LOXL4	TSS1500
cg00352218	0.18	7.05 x 10 <sup>-7</sup>	0.061	6	19,691,654	Intergenic	IGR
cg07973246	0.17	1.20 x 10 <sup>-6</sup>	0.094	12	64,238,719	SRGAP1	Body
cg24764861	-0.17	1.34 x 10 <sup>-6</sup>	0.095	16	1,495,122	CCDC154	TSS1500
cg11923320	0.13	1.47 x 10 <sup>-6</sup>	0.095	1	63,783,977	Intergenic	IGR
cg14345857	0.16	1.62 x 10 <sup>-6</sup>	0.096	5	72,742,869	FOXD1	1st exon
cg25911023	-0.14	1.73 x 10 <sup>-6</sup>	0.096	1	202,776,454	KDM5B	Body
cg01144764	-0.26	2.34 x 10 <sup>-6</sup>	0.121	10	121,633,063	C10orf119	TSS1500
cg24424115	-0.13	2.64 x 10 <sup>-6</sup>	0.129	3	58,476,822	KCTD6	TSS1500
cg18190847	0.17	4.60 x 10 <sup>-6</sup>	0.200	3	11,195,751	HRH1	5'UTR
cg06138439	0.09	4.62 x 10 <sup>-6</sup>	0.200	16	54,973,128	Intergenic	IGR
cg17886959	-0.16	5.58 x 10 <sup>-6</sup>	0.214	16	56,642,024	MT2A	TSS1500
cg02919861	0.2	5.80 x 10 <sup>-6</sup>	0.214	8	70,090,456	Intergenic	IGR

Abbreviations: adj. *p*, 5% FDR adjusted p-value; Body, between the ATG and the stop codon, irrespective of the presence of introns, exons, TSS, or promoters; BP, base-pair position; CHR, chromosome; gene, mapped gene according to University of California Santa Cruz (UCSC) RefSeq annotation; Gene region, Gene region feature category describing the CpG position. IGR, intergenic region; LogFC, log fold-change in NEDA versus EDA; TSS, transcription start site; TSS1500, 200–1,500 bases upstream of the TSS; 5'UTR, within the 5' untranslated region, between the TSS and the ATG translation initiation codon; 3'UTR, between the stop codon and poly A signal.

**TABLE 3. DMRs in NEDA vs. EDA Patients**

Parameter	CHR	BP Start	BP End	N CpGs	Max Delta-β	Mean Delta-β	Min FDR	Gene
DMR1	19	2,250,901	2,251,067	4	0.032	0.028	6.12 x 10 <sup>-8</sup>	AMH
DMR2	17	76,037,035	76,037,364	5	-0.031	-0.020	3.26 x 10 <sup>-8</sup>	TNRC6C
DMR3	7	56,515,666	56,516,129	5	-0.042	-0.029	1.61 x 10 <sup>-8</sup>	LOC650226
DMR4	19	22,234,980	22,235,850	8	-0.067	-0.022	6.76 x 10 <sup>-9</sup>	ZNF257

Abbreviations: CHR, chromosome; BP start, basepair start position; BP end, basepair end position describe the genomic coordinates of the DMR (reference: GRCh37/hg19); N CpGs, number of CpGs composing the region; Max Delta-β and Mean Delta-β, show, respectively, the maximum and mean difference in methylation beta-value found in the region, with NEDA as reference. Min FDR, minimum smoothed FDR p-value. Gene, annotated gene according to UCSC RefSeq.

the NEDA-3 status at 2 years from treatment start, after adjustment for multiple testing. Our evidence of mQTL effect exerted by these variants confirms data from a previous study on more than 32,000 healthy subjects, that demonstrated a significant impact of these 3 SNPs on

methylation levels.<sup>32</sup> The minor allele (C) for the top SNP rs2240656, located at ~135 kb upstream DMR1, was associated with increased odds of reaching the NEDA-3 status at 2-year follow-up ( $p = 1.37 \times 10^{-3}$ ;  $OR_{NEDA} = 1.73$ ; meta-analysis  $I^2 = 0$ ; Figure 2) and

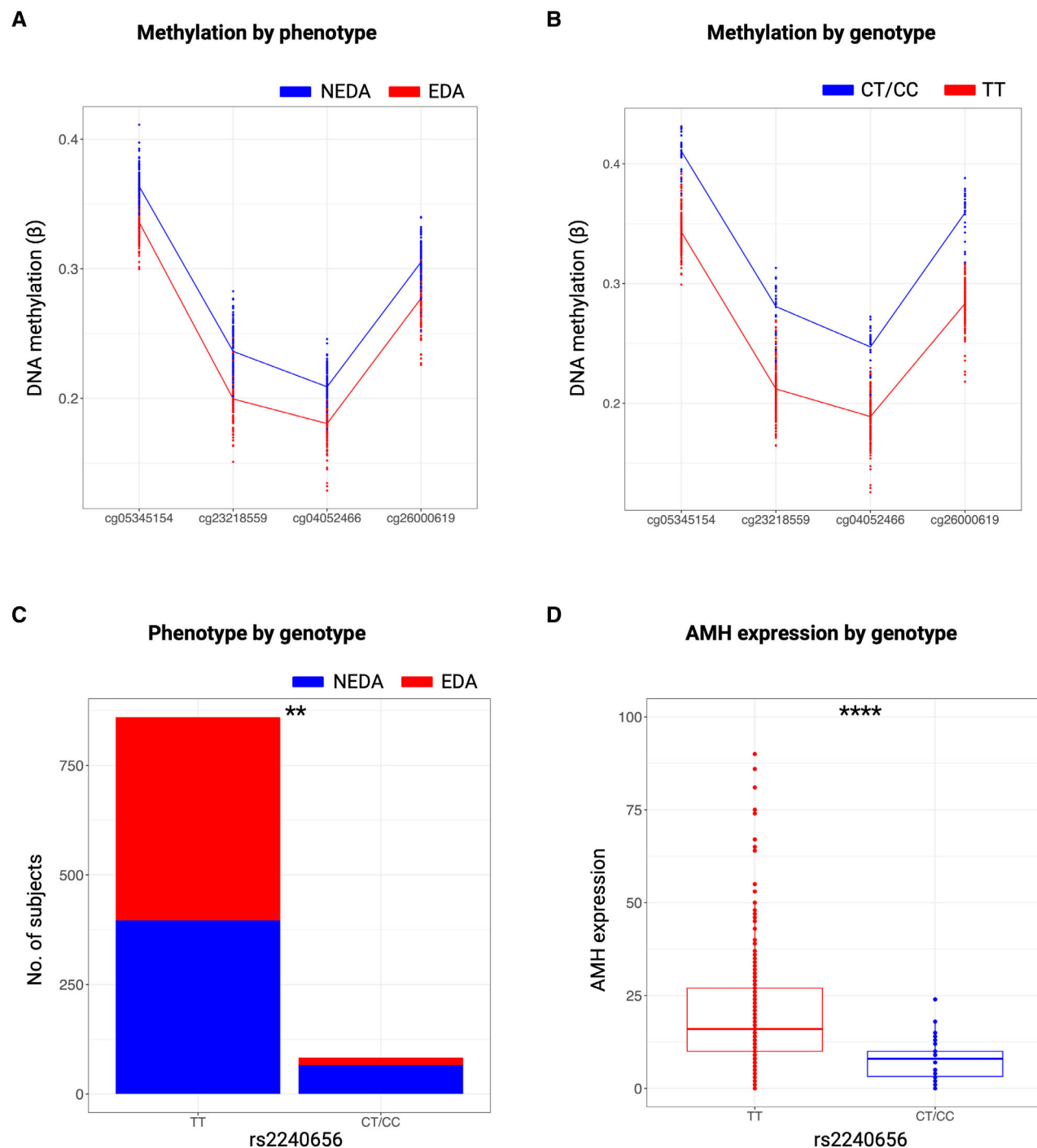


**FIGURE 2:** The DMR in *AMH* is associated with disease activity. (A) Visualization of the DMR in the *AMH* gene in NEDA versus EDA patients; on the y-axis fitted beta-values of methylation for the CpGs of the DMR1 (x-axis) are shown. (B) The effect of the genotype status of the rs2240656 SNP (the top associated SNP with disease activity) is shown, with the SNP driving the observed difference. (C) Bar plot illustrating the distribution of EDA/NEDA status across rs2240656 genotype. (D) Boxplot showing distribution of *AMH* expression levels (in gene counts) in PBMC across rs2240656 genotype. Each dot represents an individual. \*\* =  $p$ -value  $< 0.01$ ; \*\*\*\* =  $p$ -value  $< 0.0001$ . [Color figure can be viewed at [www.annalsofneurology.org](http://www.annalsofneurology.org)]



**TABLE 4. Results of the CIT**

CpG	SNP	A1	$\beta$	mQTL		OR	NEDA		CIT
				SE $\beta$	P		95% CI	p-Value	p-Value
cg23218559	rs2240656	C	0.53	0.14	$2.13 \times 10^{-4}$	1.73	1.24–2.42	0.0014	0.0197
cg04052466	rs2240656	C	0.50	0.12	$6.72 \times 10^{-5}$	1.73	1.24–2.42	0.0014	0.0255
cg26000619	rs2240656	C	0.48	0.11	$3.22 \times 10^{-5}$	1.73	1.24–2.42	0.0014	0.0267
cg23218559	rs733846	G	0.56	0.08	$5.55 \times 10^{-11}$	1.35	1.07–1.71	0.0123	0.0187
cg04052466	rs733846	G	0.59	0.06	$2.19 \times 10^{-17}$	1.35	1.07–1.71	0.0123	0.0271
cg26000619	rs733846	G	0.51	0.06	$1.96 \times 10^{-14}$	1.35	1.07–1.71	0.0123	0.0302
cg23218559	rs2074860	G	0.53	0.08	$2.52 \times 10^{-10}$	1.32	1.05–1.65	0.0157	0.0216
cg26000619	rs2074860	G	0.46	0.06	$2.76 \times 10^{-12}$	1.32	1.05–1.65	0.0157	0.0331
cg04052466	rs2074860	G	0.57	0.06	$5.67 \times 10^{-16}$	1.32	1.05–1.65	0.0157	0.0333

*Note:* The table shows the list of the CpGs that mediate the genetic risk of disease activity, assessed by the NEDA-3 status. For each CpG, the effect allele (A1) of the SNPs with the respective regression coefficients ( $\beta$ ), standard errors ( $\beta$  mQTL), and *p*-values of the mQTL effect are shown, as well as the odds ratio (OR), 95% confidence interval (95% CI), and *p*-values of association between the SNPs and the NEDA-3 status. In the rightmost column, the *p*-values from CIT are reported. Threshold for multiple testing correction for the *p* values of association with the NEDA3-status was set at  $p < 0.0167$  (0.05/3 LD blocks), as described in the main text.

with increased methylation levels of all the 4 CpGs composing DMR1 (Table S4, Table 4). This finding is consistent with our observation that NEDA subjects had higher methylation levels in this region. The DMR1 is a 167 base-pairs wide region which we found to be hypermethylated in NEDA patients and hypomethylated in EDA patients. The region maps to the bivalent promoter of the anti-Mullerian hormone (*AMH*) gene in PBMC, and specifically in CD4 and CD8 T lymphocytes (but not in B cells and monocytes), prompting a complex regulatory role on gene expression (Figure 1). In addition, *AMH* was found to be significantly expressed in brain tissue in the GTEx project,<sup>33</sup> as well as, to a lesser extent, in CD4 and CD8 cells,<sup>34</sup> as said. Interestingly, when running a GO enrichment analysis on the top 100 DMP, we found terms as, ‘Fertilization’ and ‘Reproductive system development’, together with ‘Leukocyte differentiation’, although not statistically significant after multiple testing correction (Table S9).

### Sensitivity Analysis

Given the role of *AMH* in reproductive biology, to rule out a potential bias given by the biological sex of patients (even though we had already included sex as a covariate) we run a sensitivity analysis of the DMR separately in males and females, which did not yield to the identification of the DMR in the *AMH* gene, or of any other DMR. This finding, which is probably a consequence

of reduced statistical power when analyzing separately males and females, supports that identified DMR could be important in MS patients, independent of their biological sex.

In addition, we were interested in exploring whether the difference in methylation in the *AMH* gene region was also observed when dissecting the NEDA-3 status in the 3 elements on which it is based (i.e., relapses, MRI activity, and EDSS progression), to investigate whether 1 or more of these components are mainly driving the observed difference. Therefore, we repeated the same differential methylation analysis considering separately the occurrence of relapses, the MRI activity and the EDSS progression as clinical outcomes. We observed that the reduced methylation levels of the 4 CpGs composing the DMR in *AMH* had the same direction of effects when considering separately the 3 components of the NEDA status, however the signal was stronger and statistically significant only when looking at the MRI activity (presence of new/enlarging or contrast-enhancing lesions) over the 2-year follow-up (Table S10).

### DNA Methylation in *AMH* Mediates the Genetic Risk of Disease Activity

We found that genetic variation affects both DNA methylation in the *AMH* gene and the risk of disease activity, but it remains to be clarified whether the SNPs primarily affect the levels of DNA methylation, which then mediate

an increased risk of disease activity (i.e., methylation is a mediator of the genetic risk of disease activity), or if the SNPs affect independently methylation and the risk of disease activity. To answer this question, we used causal inference testing (CIT), as previously reported.<sup>12,27</sup> We run CIT on the 3 SNPs with evidence of mQTL effect and association with risk of disease activity, finding evidence that for all the SNPs DNA methylation is the mediator of their effect on disease activity ( $p < 0.05$ ) (Table 4).

**Increased DNA Methylation Levels in the DMR Lead to Decreased AMH Expression.** Modulating the levels of DNA methylation in a promoter region is likely to provoke changes in gene expression.<sup>4</sup> Therefore, we verified whether the SNPs that affect the risk of disease activity through modulation of DNA methylation in the *AMH* gene had also an impact on gene expression. To do so, we used RNA-seq data from PBMC from 225 patients involved in the methylation analysis. We found that all the 3 SNPs were associated with lower *AMH* expression in PBMC (rs2240656:  $\beta = -0.87$ , SE 0.16,  $P = 1.1 \times 10^{-7}$ ; rs733846:  $\beta = -0.58$ , SE = 0.091,  $P = 1.38 \times 10^{-9}$ ; rs2074860:  $\beta = -0.71$ , SE = 0.92,  $P = 5.9 \times 10^{-13}$ ) (Figure 2D). Then, we conducted a MR analysis to assess causality between methylation and expression and to exclude reverse causation. The results confirm that higher methylation levels in the DMR driven by genotype is causally associated with decreased *AMH* expression ( $p < 0.0001$ ;  $\beta = -1.47$  for decrease in gene expression for increase of 1-unit of methylation  $M$ -values, SE 0.06), further clarifying mechanistically the events that lead to increased risk of disease activity in patients who are carriers of the risk alleles for the mentioned SNPs.

## Discussion

In this work, we studied the impact of the peripheral immune methylome on disease activity in RR-MS, assessed with the NEDA-3 status. First, we investigated single CpGs, and found 7 DMP that were significantly associated with disease activity, after correction for multiple testing. Although instrumental to the generation of DMR, the DMP analysis yielded some interesting associations, which is worth to briefly comment. As an example, the top associated CpG (cg27267436) maps to an intronic region of *APBA3* (amyloid beta precursor protein binding family A member 3), also known as *MINT3*. *APBA3/MINT3* is an activator of the hypoxia-inducible factor 1- $\alpha$  (*HIF1A*) gene,<sup>35</sup> through which it plays an important role in the formation of beta-amyloid plaques in Alzheimer disease<sup>36</sup> and in the activation of monocytes and macrophages.<sup>35</sup> *HIF1A* is not only a fundamental driver of Alzheimer disease pathobiology,<sup>37</sup> but it is also

essential for the Th17/regulatory T cell balance, and *HIF1A* knock-out mice do not develop Experimental Autoimmune Encephalitis, an animal model of MS.<sup>38</sup> Cg20308351 maps to *CARD11* (caspase recruitment domain family member 11), and a previous study found a region in *CARD11* which is differentially methylated in B cells of MS patients versus controls.<sup>39</sup> *CARD11* regulates *NF- $\kappa$ B* through *BCL10* in B cells,<sup>40</sup> and represents 1 of the main molecular targets of the Bruton tyrosine kinase inhibitors (BTKi), a class of drugs that is currently under investigation as DMT for MS.

Next, we focused on the analysis of DMR, as it is known that differences in methylation occurring in clusters of neighboring CpGs have a more relevant biological meaning, and reduce the risk of false positives.<sup>41</sup> We identified 4 regions that were differentially methylated in NEDA versus EDA patients, mapping to 4 genes (*AMH*, *TNRC6C*, *LOC650226*, *ZNF257*), as shown in Table 3. Hypothesizing that the observed differences in DNA methylation may be an effect of the underlying genetic variation, we studied the mQTL effect exerted by nearby SNPs, finding that all the DMR are consistently affected by genetic variants. To better support this connection, we verified whether the variants themselves associate with disease activity, conducting a genetic association study on a cohort of 1,408 MS patients. In this analysis, SNPs modulating the levels of methylation in only 1 of the 4 DMR, mapping to the *AMH* gene, resulted to be associated with disease activity. Next, to provide an insight on the underlying mechanisms, we tested whether DNA methylation can mediate the genetic risk for disease activity exerted by SNPs in *AMH*. Our data demonstrated that SNPs alleles that reduce the risk of disease activity act through an increase in DNA methylation in the bivalent promoter of the *AMH* gene in the immune cells, which consequently results in lower *AMH* expression in PBMC (Figure 2).

The AMH is a fundamental sex hormone of the transforming growth factor beta (TGF- $\beta$ ) family, a key regulator of the immune system, and has known effects during fetal development and adult life, with a role both in males and females. During fetal life, higher expression of the *AMH* gene prevents the development of a female reproductive tract. Recent evidence highlighted that the AMH continues to exert important effects during the adult life as well, reflecting the aging of the reproductive system.<sup>42,43</sup> In adult women, AMH decreases together with the number of follicles over the time, hence its role as a marker in conditions like the polycystic ovarian syndrome.<sup>42</sup> In men, the AMH is produced by the Sertoli cells in the testis during sex differentiation and it is suppressed by androgens when the primary differentiation is completed.<sup>43</sup> At puberty, AMH levels rise again in the

male and regulate fertility, whereas they decrease with the aging of the reproductive system.<sup>43</sup>

Hormonal factors are crucial for MS. Specifically, gender difference significantly impacts MS, which is more common in women but, once established, the disease course seems to be less favorable in men. In women, physiological conditions related to changes in sex hormones (as pregnancy, post-partum, or menopause) significantly influence the risk of relapses and disease outcomes.<sup>44,45</sup> However, the biological mechanisms underlying the importance of sex hormones in MS are still not completely understood.<sup>46</sup> Interestingly, the AMH is most well-known for the mentioned effects on the reproductive systems, but it is also part of the TGF- $\beta$  superfamily, a key player in development and tolerance of the immune system.<sup>47</sup> Nevertheless, the possible involvement of AMH in immune mechanisms is not clear, but some studies report an increased risk of autoimmunity with ovarian dysfunction and AMH dysregulation.<sup>47</sup> Moreover, very little is known about AMH and MS,<sup>46</sup> as the few previous small studies that assessed the association of AMH levels and disease outcomes in MS overall led to controversial results.<sup>48–50</sup>

In the present study, we found that the genetic background influences the levels of disease activity in MS acting through changes in DNA methylation that lead to modulation of *AMH* expression. As said, the circulating levels of AMH reflect aging. It is very well known that a younger age is a strong risk factor for clinical and radiological signs of new inflammatory disease activity, while with aging such risk decreases.<sup>51</sup> On this basis, our findings may underline the importance of hormonal factors in the machinery of the so-called ‘inflammaging’, which is thought to play a major role in MS.<sup>52</sup> This hypothesis, however, requires further support from future functional studies. Interestingly, when we run a GO enrichment analysis, we found an enrichment for many terms related with in utero development, fertilization, and embryogenic development, involving other genes (Table S9). These data additionally support that sex hormones are important in determining disease activity in MS and prompt future interventional studies that focus on related lifestyle and modifiable factors.

### Limitations of This Study

The present study presents some limitations that should be highlighted; the more relevant is the retrospective collection of clinical data to group patients according to the NEDA-3 status. We acknowledge this limitation, as prospective data collection is certainly the gold standard in clinical studies. However, we believe also that this type of study could provide a realistic perspective outside clinical trials, making the results more directly linked to routine

clinical practice and real life management. Similarly, the retrospective study design did not allow to obtain measures of brain atrophy at MRI, as it is not part of the routine clinical assessment of patients. Future follow-up investigations should also be focused on assessing potential association with brain atrophy. Another limitation is represented by the sample size of the cohort used in the genetic association study on the NEDA-3 status. In this case, the relatively small sample size for a genetic association analysis may have reduced the number of significant variants for which an association with the NEDA-3 status was found. We are aware of this issue, and therefore we used a stringent statistical approach with multiple testing correction as reported in the Methods, to minimize the possibility of false positive associations. Another limitation is the lack of an additional validation dataset to replicate our results, which would strengthen our findings. Multi-center studies using multi-layer molecular information are the ideal setting to translate research findings into the bedside practice. However, harmonization of complex clinical datasets (as the one used in our study) between multiple centers is often extremely challenge and can prevent the feasibility of this kind of efforts.

### Conclusions

In conclusions, this work unraveled a novel molecular pathway that is relevant to disease severity implicating the interaction between the genetic background and DNA methylation in *AMH*, and adds more evidence to the importance of sex hormones in the pathobiology of MS.

### Acknowledgments

The present study is part of the FindingMS project, which was supported by ERA PerMed-JTC2018 (co-funded by the European Commission). Open access funding provided by BIBLIOSAN.

### Potential Conflicts of Interest

Nothing to report.

### Authors Contributions

A.G., F.C., M.S., R.L., and F.E. contributed to the conception and design of the study; A.G., B.P., E.M., F.C., M.S., K.M., F.B., L.F., L.M., and F.E. contributed to the acquisition and analysis of data; A.G., E.M., F.C., M.S., R.L., M.F., and F.E. contributed to drafting the text or preparing the figures.

## Data Availability

Anonymized data of the analyses presented in this study are available upon reasonable request to the corresponding author.

## References

- Thompson AJ, Baranzini SE, Geurts J, et al. Multiple sclerosis. *Lancet* 2018;391:1622–1636. [https://doi.org/10.1016/S0140-6736\(18\)30481-1](https://doi.org/10.1016/S0140-6736(18)30481-1).
- Confavreux C, Vukusic S, Moreau T, Adeleine P. Relapses and progression of disability in multiple sclerosis. *N Engl J Med* 2000;343:1430–1438. <https://doi.org/10.1056/NEJM200011163432001>.
- Mattei AL, Bailly N, Meissner A. DNA methylation: a historical perspective. *Trends Genet* 2022;38:676–707. <https://doi.org/10.1016/j.tig.2022.03.010>.
- Weber M, Hellmann I, Stadler MB, et al. Distribution, silencing potential and evolutionary impact of promoter DNA methylation in the human genome. *Nat Genet* 2007;39:457–466. <https://doi.org/10.1038/ng1990>.
- Klutstein M, Nejman D, Greenfield R, Cedar H. DNA methylation in cancer and aging. *Cancer Res* 2016;76:3446–3450. <https://doi.org/10.1158/0008-5472.CAN-15-3278>.
- Olsson T, Barcellos LF, Alfredsson L. Interactions between genetic, lifestyle and environmental risk factors for multiple sclerosis. *Nat Rev Neurol* 2017;13:25–36. <https://doi.org/10.1038/nrneurol.2016.187>.
- Zheleznyakova GY, Piket E, Marabita F, et al. Epigenetic research in multiple sclerosis: progress, challenges, and opportunities. *Physiol Genomics* 2017;49:447–461. <https://doi.org/10.1152/physiolgenomics.00060.2017>.
- Kulakova OG, Kabilov MR, Danilova LV, et al. Whole-genome DNA methylation analysis of peripheral blood mononuclear cells in multiple sclerosis patients with different disease courses. *Acta Naturae* 2016;8:103–110.
- Marabita F, Almgren M, Sjöholm LK, et al. Smoking induces DNA methylation changes in multiple sclerosis patients with exposure-response relationship. *Sci Rep* 2017;7:14589. <https://doi.org/10.1038/s41598-017-14788-w>.
- Maltby VE, Graves MC, Lea RA, et al. Genome-wide DNA methylation profiling of CD8+ T cells shows a distinct epigenetic signature to CD4+ T cells in multiple sclerosis patients. *Clin Epigenetics* 2015;7:118. <https://doi.org/10.1186/s13148-015-0152-7>.
- Bos SD, Page CM, Andreassen BK, et al. Genome-wide DNA methylation profiles indicate CD8+ T cell hypermethylation in multiple sclerosis. *Plos One* 2015;10:e0117403. <https://doi.org/10.1371/journal.pone.0117403>.
- Kular L, Liu Y, Ruhrmann S, et al. DNA methylation as a mediator of HLA-DRB1\*15:01 and a protective variant in multiple sclerosis. *Nat Commun* 2018;9:2397. <https://doi.org/10.1038/s41467-018-04732-5>.
- Pidsley R, Zotenko E, Peters TJ, et al. Critical evaluation of the Illumina MethylationEPIC BeadChip microarray for whole-genome DNA methylation profiling. *Genome Biol* 2016;17:208. <https://doi.org/10.1186/s13059-016-1066-1>.
- Aryee MJ, Jaffe AE, Corrada-Bravo H, et al. Minfi: a flexible and comprehensive Bioconductor package for the analysis of Infinium DNA methylation microarrays. *Bioinformatics* 2014;30:1363–1369. <https://doi.org/10.1093/bioinformatics/btu049>.
- Lê S, Josse J, Husson F. FactoMineR: an R package for multivariate analysis. *J Stat Softw* 2008;25:1–18. <https://doi.org/10.18637/jss.v025.i01>.
- Sun Z, Chai HS, Wu Y, et al. Batch effect correction for genome-wide methylation data with Illumina Infinium platform. *BMC Med Genomics* 2011;4:84. <https://doi.org/10.1186/1755-8794-4-84>.
- Ross JP, Van Dijk S, Phang M, et al. Batch-effect detection, correction and characterisation in Illumina HumanMethylation450 and MethylationEPIC BeadChip array data. *Clin Epigenetics* 2022;14:58. <https://doi.org/10.1186/s13148-022-01277-9>.
- Leek JT, Scharpf RB, Bravo HC, et al. Tackling the widespread and critical impact of batch effects in high-throughput data. *Nat Rev Genet* 2010;11:733–739. <https://doi.org/10.1038/nrg2825>.
- Zheng SC, Breeze CE, Beck S, Teschendorff AE. Identification of differentially methylated cell types in epigenome-wide association studies. *Nat Methods* 2018;15:1059–1066. <https://doi.org/10.1038/s41592-018-0213-x>.
- Ritchie ME, Phipson B, Wu D, et al. Limma powers differential expression analyses for RNA-seq and microarray studies. *Nucleic Acids Res* 2015;43:e47. <https://doi.org/10.1093/nar/gkv007>.
- Peters TJ, Buckley MJ, Chen Y, et al. Calling differentially methylated regions from whole genome bisulphite sequencing with DMRcate. *Nucleic Acids Res* 2021;49:e109. <https://doi.org/10.1093/nar/gkab637>.
- Liao Y, Wang J, Jaehnig EJ, et al. WebGestalt 2019: gene set analysis toolkit with revamped UIs and APIs. *Nucleic Acids Res* 2019;47:W199–W205. <https://doi.org/10.1093/nar/gkz401>.
- Chang CC, Chow CC, Tellier LC, et al. Second-generation PLINK: rising to the challenge of larger and richer datasets. *GigaScience* 2015;4:7. <https://doi.org/10.1186/s13742-015-0047-8>.
- The 1000 Genomes Project Consortium, Corresponding authors, Auton A, Brooks LD, et al. A global reference for human genetic variation. *Nature* 2015;526:68–74. <https://doi.org/10.1038/nature15393>.
- Gabriel SB, Schaffner SF, Nguyen H, et al. The structure of haplotype blocks in the human genome. *Science* 2002;296:2225–2229. <https://doi.org/10.1126/science.1069424>.
- McCarthy S, Das S, Kretschmar W, et al. A reference panel of 64,976 haplotypes for genotype imputation. *Nat Genet* 2016;48:1279–1283. <https://doi.org/10.1038/ng.3643>.
- Liu Y, Aryee MJ, Padyukov L, et al. Epigenome-wide association data implicate DNA methylation as an intermediary of genetic risk in rheumatoid arthritis. *Nat Biotechnol* 2013;31:142–147. <https://doi.org/10.1038/nbt.2487>.
- Liao Y, Smyth GK, Shi W. featureCounts: an efficient general purpose program for assigning sequence reads to genomic features. *Bioinformatics* 2014;30:923–930. <https://doi.org/10.1093/bioinformatics/btt656>.
- Ewels P, Magnusson M, Lundin S, Käller M. MultiQC: summarize analysis results for multiple tools and samples in a single report. *Bioinformatics* 2016;32:3047–3048. <https://doi.org/10.1093/bioinformatics/btw354>.
- Banwell B, Giovannoni G, Hawkes C, Lublin F. Editors' welcome and a working definition for a multiple sclerosis cure. *Mult Scler Relat Disord* 2013;2:65–67. <https://doi.org/10.1016/j.msard.2012.12.001>.
- Roadmap Epigenomics Consortium, Kundaje A, Meuleman W, et al. Integrative analysis of 111 reference human epigenomes. *Nature* 2015;518:317–330. <https://doi.org/10.1038/nature14248>.
- Min JL, Hemani G, Hannon E, et al. Genomic and phenotypic insights from an atlas of genetic effects on DNA methylation. *Nat Genet* 2021;53:1311–1321. <https://doi.org/10.1038/s41588-021-00923-x>.
- Lonsdale J, Thomas J, Salvatore M, et al. The genotype-tissue expression (GTEx) project. *Nat Genet* 2013;45:580–585. <https://doi.org/10.1038/ng.2653>.
- Schmiedel BJ, Singh D, Madrigal A, et al. Impact of genetic polymorphisms on human immune cell gene expression. *Cell* 2018;175:1701–1715.e16. <https://doi.org/10.1016/j.cell.2018.10.022>.

35. Hara T, Nakaoka HJ, Hayashi T, et al. Control of metastatic niche formation by targeting APBA3/Mint3 in inflammatory monocytes. *Proc Natl Acad Sci* 2017;114:E4416–E4424. <https://doi.org/10.1073/pnas.1703171114>.
36. Caster AH, Kahn RA. Recruitment of the Mint3 adaptor is necessary for export of the amyloid precursor protein (APP) from the Golgi complex. *J Biol Chem* 2013;288:28567–28580. <https://doi.org/10.1074/jbc.M113.481101>.
37. March-Diaz R, Lara-Ureña N, Romero-Molina C, et al. Hypoxia compromises the mitochondrial metabolism of Alzheimer's disease microglia via HIF1. *Nat Aging* 2021;1:385–399. <https://doi.org/10.1038/s43587-021-00054-2>.
38. Dang EV, Barbi J, Yang HY, et al. Control of TH17/Treg balance by hypoxia-inducible factor 1. *Cell* 2011;146:772–784. <https://doi.org/10.1016/j.cell.2011.07.033>.
39. Maltby VE, Lea RA, Graves MC, et al. Genome-wide DNA methylation changes in CD19+ B cells from relapsing-remitting multiple sclerosis patients. *Sci Rep* 2018;8:17418. <https://doi.org/10.1038/s41598-018-35603-0>.
40. Sommer K, Guo B, Pomerantz JL, et al. Phosphorylation of the CARMA1 linker controls NF- $\kappa$ B activation. *Immunity* 2005;23:561–574. <https://doi.org/10.1016/j.immuni.2005.09.014>.
41. Rakyan VK, Down TA, Balding DJ, Beck S. Epigenome-wide association studies for common human diseases. *Nat Rev Genet* 2011;12:529–541. <https://doi.org/10.1038/nrg3000>.
42. Dewailly D, Andersen CY, Balen A, et al. The physiology and clinical utility of anti-Müllerian hormone in women. *Hum Reprod Update* 2014;20:370–385. <https://doi.org/10.1093/humupd/dmt062>.
43. Xu HY, Zhang HX, Xiao Z, et al. Regulation of anti-Müllerian hormone (AMH) in males and the associations of serum AMH with the disorders of male fertility. *Asian J Androl* 2019;21:109–114. [https://doi.org/10.4103/aja.aja\\_83\\_18](https://doi.org/10.4103/aja.aja_83_18).
44. Confavreux C, Hutchinson M, Hours MM, et al. Rate of pregnancy-related relapse in multiple sclerosis. *N Engl J Med* 1998;339:285–291. <https://doi.org/10.1056/NEJM199807303390501>.
45. Dobson R, Jokubaitis VG, Giovannoni G. Change in pregnancy-associated multiple sclerosis relapse rates over time: a meta-analysis. *Mult Scler Relat Disord* 2020;44:102241. <https://doi.org/10.1016/j.msard.2020.102241>.
46. Ysrraelit MC, Correale J. Impact of sex hormones on immune function and multiple sclerosis development. *Immunology* 2019;156:9–22. <https://doi.org/10.1111/imm.13004>.
47. Visser JA, Schipper I, Laven JSE, Themmen APN. Anti-Müllerian hormone: an ovarian reserve marker in primary ovarian insufficiency. *Nat Rev Endocrinol* 2012;8:331–341. <https://doi.org/10.1038/nrendo.2011.224>.
48. Thöne J, Kollar S, Noursome D, et al. Serum anti-Müllerian hormone levels in reproductive-age women with relapsing–remitting multiple sclerosis. *Mult Scler J* 2015;21:41–47. <https://doi.org/10.1177/1352458514540843>.
49. Sepúlveda M, Ros C, Martínez-Lapiscina EH, et al. Pituitary-ovary axis and ovarian reserve in fertile women with multiple sclerosis: a pilot study. *Mult Scler J* 2016;22:564–568. <https://doi.org/10.1177/1352458515602339>.
50. Graves JS, Henry RG, Cree BAC, et al. Ovarian aging is associated with gray matter volume and disability in women with MS. *Neurology* 2018;90:e254–e260. <https://doi.org/10.1212/WNL.0000000000004843>.
51. Confavreux C, Vukusic S. Age at disability milestones in multiple sclerosis. *Brain* 2006;129:595–605. <https://doi.org/10.1093/brain/awh714>.
52. Perdaens O, Van Pesch V. Molecular mechanisms of Immunosenescence and Inflammaging: relevance to the immunopathogenesis and treatment of multiple sclerosis. *Front Neurol* 2022;12:811518. <https://doi.org/10.3389/fneur.2021.811518>.